

Unstructured intermediate states in single protein force experiments

Ivan Junier and Felix Ritort*

*Departament de Física Fonamental, Facultat de Física,
Universitat de Barcelona, Diagonal 647, 08028 Barcelona, Spain*

Recent single-molecule force measurements on single-domain proteins have highlighted a three-state folding mechanism where a stabilized intermediate state (\mathcal{I}) is observed on the folding trajectory between the stretched state and the native state. Here we investigate on-lattice protein-like heteropolymer models that lead to a three-state mechanism and show that force experiments can be useful to determine the structure of \mathcal{I} . We have mostly found that \mathcal{I} is composed of a core stabilized by a high number of native contacts, plus an unstructured extended chain. The lifetime of \mathcal{I} is shown to be sensitive to modifications of the protein that spoil the core. We then propose three types of modifications –point mutations, cuts and circular permutations– aiming at: 1) confirming the presence of the core and 2) determining its location, within one amino acid accuracy, along the polypeptide chain. We also propose force jump protocols aiming to probe the on/off-pathway nature of \mathcal{I} .

Keywords: single molecule experiments — protein folding — kinetic intermediates — unstructured proteins — on-lattice models

The recent development of single molecule experimental tools [1, 2, 3] has allowed to investigate the fundamental biochemical and biophysical processes occurring at a molecular level inside the cell [4]. For instance, the folding of proteins [5, 6, 7, 8] can nowadays be studied by manipulating *one* protein at a time [4]. Examples are the titin molecule pulled by AFM [9, 10] or the *E. coli* 155-residues RNase H protein [12, 13] pulled by optical tweezers [11]. At low denaturant concentration, FRET measurements have shown the presence of highly compact denaturated states [12, 13] whose existence was expected from previous bulk experiments [14]. The latter suggests a hierarchical folding mechanism where the folding of the protein to the native state is preceded by a fast collapse of the most stable region of the native structure. The formation of a structure that has a short lifetime and many native contacts has been observed during the folding of many single-domain proteins [5, 15]. On the other hand, recent experiments using optical tweezers have investigated the unfolding/folding transition of the RNase H protein under the action of a mechanical force applied at the two ends of the molecule [11]. These experiments show the stabilization of an intermediate state at forces around 5pN [11]. The protein is observed to exist in three different states: the stretched (\mathcal{S}), the intermediate (\mathcal{I}) and the native (\mathcal{N}) states¹. Using thermodynamic considerations it has been argued that \mathcal{I} is identical to the early state (\mathcal{E}) that forms at zero force and room temperature [11]. The experimental results also suggest that \mathcal{I} is an obligatory step in the folding pathway from \mathcal{S} to \mathcal{N} , hereafter referred to as an intermediate *on-pathway*.

The determination of the structure of generic unstructured states, i.e. that lack a well-structured three-

dimensional fold, is a major experimental challenge in modern biophysics. A well-known example is the molten-globule state sometimes observed in thermal denaturation in proteins [5]. The identification of the unstructured states is limited by their large structural fluctuations that make usual techniques (X-ray or NMR) poorly predictive. On the other hand, growing evidence shows that a large number of proteins are intrinsically unstructured and contain a fair amount of disordered regions [16]. The use of new experimental techniques aiming to probe unstructured states is therefore a question of great interest.

Is there any connection between the intermediate states that have been detected in AFM and optical tweezers experiments and the intrinsically disordered states observed in many proteins? Is it possible to extract useful information about the structure of the intermediate state observed in single molecule pulling experiments by designing specific experimental protocols?. To address such questions we use a phenomenological approach based on the numerical investigation of on-lattice heteropolymers in the presence of mechanical force [17]. This class of models contain the minimal number of ingredients necessary to capture the basic phenomenology (thermodynamics and kinetics) of the folding transition problem. In addition, they are simple enough to allow exhaustive statistical studies that are difficult to carry out with other more accurate and realistic descriptions of proteins. In contrast to simple two-state models, on-lattice heteropolymers are phenomenological models where the molecular extension that reflects the internal configuration of the protein is the natural reaction coordinate [18].

By introducing mechanical force in the analysis [19], we show how it is possible to reproduce and interpret the three-state behavior observed in the experiments. We numerically investigate several topologies of the native structure and find that they generally lead to a three-state scenario in the presence of mechanical force. The new intermediate state (\mathcal{I}) is typically composed of a

*To whom correspondence should be sent: ritort@ffn.ub.es

¹ Abbreviations: \mathcal{N} , native state; \mathcal{I} , intermediate state; \mathcal{S} , stretched state; \mathcal{E} , early state.

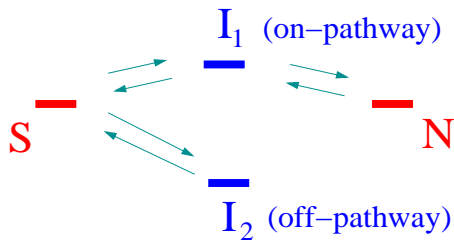


FIG. 1: Kinetic scheme of a folding reaction with different types of intermediate states. \mathcal{I}_2 is off-pathway (misfolded) since it is not directly connected to \mathcal{N} whereas \mathcal{I}_1 is on-pathway.

compact core with a high number of native contacts, plus an unstructured extended chain. Moreover, \mathcal{I} is not necessarily identical to the early state (\mathcal{E}) that forms when folding at zero force.

We then show how the structure of the intermediate state \mathcal{I} , that has been observed in single molecule pulling experiments, can be determined by means of specific experimental protocols that have been used in protein biophysics in different contexts. We propose experimental single protein force protocols that introduce modifications in the amino acid sequence of the protein to infer information about the structure of \mathcal{I} . We propose three techniques based on i) single amino acid mutations, ii) cutting off the polypeptide chain at various lengths and iii) circular permutations of the protein. These techniques lead to the location of the core due to the fact that the system $\mathcal{S} \leftrightarrow \mathcal{I}$ undergoes a transition when the modifications involve amino acids of the core. These protocols could be also used in the future to unveil the local structure of globally unstructured proteins that contain a mixture of disordered and ordered regions [16].

Finally, by investigating the folding kinetics at different solvent conditions, we have also found the presence of other intermediate states that, we show, are misfolded states (Fig. 1). In contrast with on-pathway states, misfolded states are *off-pathway*: starting from such state, the folding pathway to \mathcal{N} must pass through \mathcal{S} . Although off-pathway and on-pathway states may be hard to distinguish (e.g. when they have the same molecular extension), we show that a force jump protocol is useful to quantify the fraction of on/off-pathway trajectories that lead to on/off pathway states respectively.

I. THREE-STATE PROTEINS

Following the sequence optimization procedure of Shakhnovich and Gutin [17], we design heteropolymers on a cubic lattice that fold into a *unique* compact structure (Fig. 2). The heteropolymer consists of a chain of monomers indexed by i ($1 \leq i \leq N$) with nearest neigh-

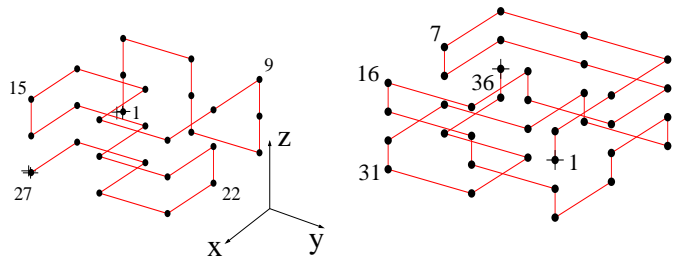
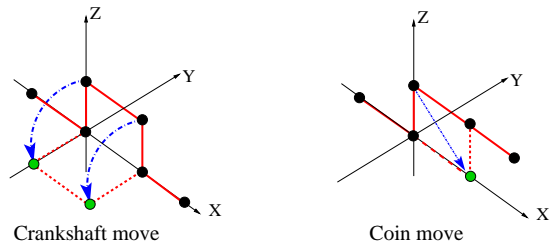


FIG. 2: Two archetypal native topologies of designed heteropolymers on a cubic lattice. Left: Structure \mathcal{S}_1 , $N = 27$. Right: Structure \mathcal{S}_2 , $N = 36$. The numbers indicate the positions n of the monomers along the chain. The crosses indicate the two ends of the chain.

bor pair interactions E_{ij} between monomers i, j that are not contiguous along the chain. The values of E_{ij} , which determine the native configuration, are obtained following an optimization algorithm [17] starting from an initial set of interactions E_{ij}^0 and a given topology of the native structure, i.e. a given chain configuration in \mathcal{N} . We note that, by definition of the model, several sets of interactions E_{ij} can be associated to identical topologies of the native state. The values of E_{ij}^0 , and hence of E_{ij} , are drawn from a Gaussian distribution of zero mean and variance Δ^2 . Δ is measured in units of $k_B T^*$ where k_B is the Boltzmann constant and T^* is a reference temperature that we fix to 300K. The dynamics of the heteropolymer consists in the standard "coin and crankshaft" Monte-Carlo dynamics with Metropolis rates [20] (elementary moves are shown in the illustration). Note that these types of moves might not be optimally suited for pulling experiments since they transmit stress very slowly over long straight chains. However, we still expect that the generality of our results goes beyond the details of the local dynamics we use for the on-lattice heteropolymers.



The timescale is fixed by the unit of Monte-Carlo steps that we set to 100 ns, a value that leads to results in quantitative agreement with experimental results (e.g. [11]). In this type of model, the values of E_{ij} correspond to specific short-range tertiary contacts along the protein chain. Although long-range interactions, side-chain interactions and other short-scale details of proteins (such as the secondary structural motifs) are not included in the model, such designed heteropolymers have been shown to dis-

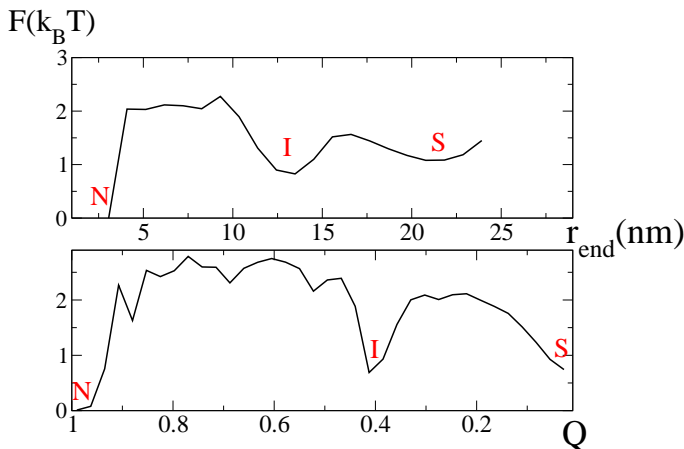


FIG. 3: Free energy profiles projected along r_{end} and Q for the structure \mathbf{S}_2 . $\Delta = 1.2 k_B T^*$ and $f = 9$ pN. Three main states can be defined: the native state (\mathcal{N}), an intermediate state (\mathcal{I}) and the stretched state (\mathcal{S}). They correspond to the deeper local minima along the free energy profiles. The values for r_{end} and Q have been averaged over $10\mu\text{s}$.

play folding properties that are similar to those of single-domain proteins [17]. The results we show here are quite general and have been reproduced with different native structures. However, for the sake of clarity, throughout this paper we present results for two archetypal compact structures \mathbf{S}_1 , \mathbf{S}_2 (Fig. 2) whose sizes are respectively $N = 27, 36$. These correspond to small globular proteins with a number of residues in the range of $50 - 100$ [21].

To characterize the state of the heteropolymer, we monitor the temporal evolution of the end-to-end distance r_{end} of the molecule and the percentage of native contacts Q ($0 \leq Q \leq 1$). The lattice spacing is set equal to 1 nm for the heteropolymer to have contour lengths that are similar to those of proteins studied in experiments (e.g. [11]). A state is defined as the location of a minimum in the free energy projected along Q or r_{end} (see Fig. 3). Due to the discrete nature of the on-lattice heteropolymer, the free energy landscape along r_{end} is a rugged surface (see for instance [18]). Intermediate states then appear as highly roughed basins that can be better identified by ensemble or time averaging of the values of r_{end} and Q over a finite bandwidth. In this way, we obtain smooth free energy landscapes in space and Q with well defined minima (see Fig. 3). Small single-domain proteins are commonly described as two-state systems having two possible conformations: native and denatured [5]. In experiments, by varying the concentration of denaturant one finds a first-order like transition where both states coexist [5] -see however [26] for exceptions to this general result. In the presence of applied mechanical force, cooperative transitions take place between the native state \mathcal{N} and a stretched state \mathcal{S} as observed in single molecule AFM measurements in engineered polyproteins [24] and in RNA pulling experiments using optical twee-

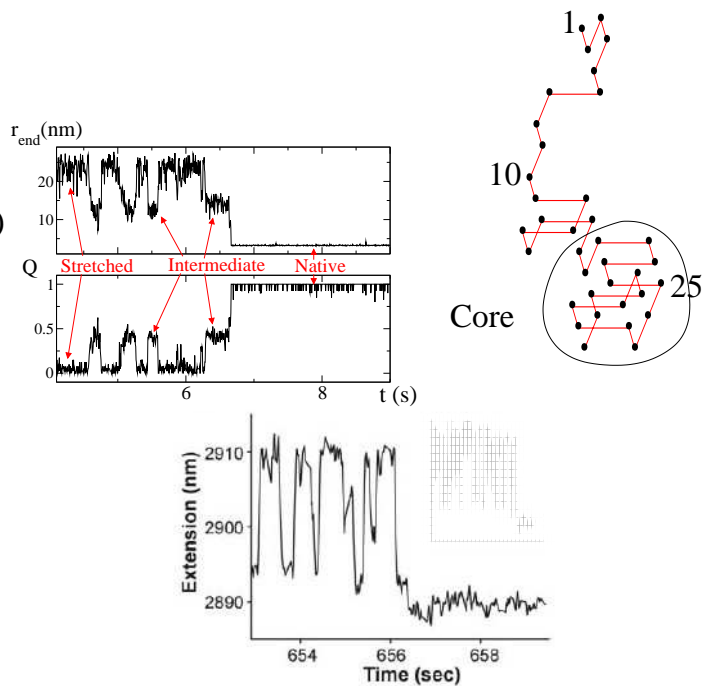


FIG. 4: Upper left: Three-state behavior in \mathbf{S}_2 . $\Delta = 1.35 k_B T^*$ and $f = 10.1$ pN. Upper right: Typical structure, composed of a core plus an extended chain, of a configuration in \mathcal{I} . Lower panel: Experimental trace of the RNase H protein at constant force ($f \sim 6$ pN) using optical tweezers (taken from [11]).

ers [25]. In order to introduce mechanical force in the lattice we must avoid the lattice anisotropy effects that act as kinetic traps for the rotational degrees of freedom [19]. To this end, we add a term of the type $-\vec{f} \cdot \vec{r}_{\text{end}}$ where \vec{f} is a force of constant modulus (measured in units of Δ/a) that is always aligned with the end-to-end vector \vec{r}_{end} of the heteropolymer [19] – see supplementary material. We have verified that a two-state system under the action of a (moderate) mechanical force leads to an exponential folding/unfolding times distribution (Fig. S1 and S2 in the Supp. Mat.).

Intermediate and misfolded states

Starting from \mathcal{S} and by further decreasing the force down to zero, a single-domain protein shows a cooperative transition to \mathcal{N} at a given value of the force. Our simulations show that several structures that exhibit a two-state behavior in a given range of temperatures, also show a three-state behavior under the action of mechanical force at lower temperatures – or equivalently at larger values of Δ at the fixed temperature T^* . In Fig. 4, we show the three-state behavior by plotting the temporal evolution of both r_{end} and Q , starting from a random ini-

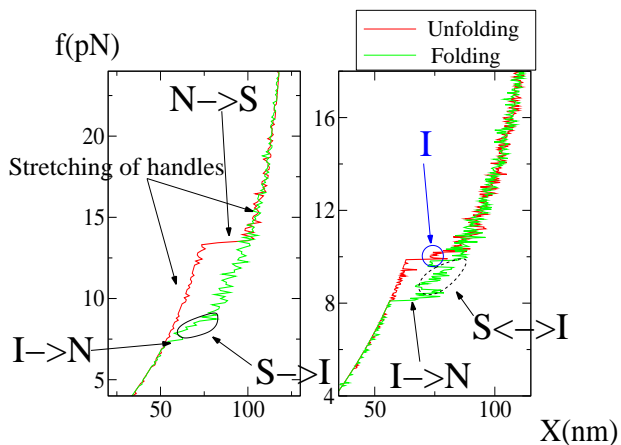


FIG. 5: Force-extension curve for S_2 with $\Delta = 1.2 k_B T^*$ in a pulling protocol with different loading rates r . Left, $r = 4 \text{ pN}\cdot\text{s}^{-1}$. Right, $r = 0.4 \text{ pN}\cdot\text{s}^{-1}$. We have included the contribution of the handles (modeled as a freely jointed chain). The total extension (protein plus handles) is equal to $X = r_{\text{end}} + x_{\text{FJC}}$ where $x_{\text{FJC}} = 100 \coth(fa/k_B T) - k_B T/f a$ corresponds to the extension of the freely jointed chain at force f . At large loading rate r , the unfolding transition $N \rightarrow S$ is of the all-or-none type [11] whereas at lower loading rates (right panel), the intermediate state \mathcal{I} along the transition (blue circle) can be resolved. At low rates, we also observe multiple transitions between S and \mathcal{I} during the refolding (black dashed circle).

tial configuration. The three-state mechanism has been observed for different matrices E_{ij} , i.e. for different energy values and different topologies of the native structure.

Fig. 4 shows that the final folding stage takes place from \mathcal{I} suggesting that \mathcal{I} is on-pathway. Sometimes, however, the transition from S to N does not go through \mathcal{I} (See Fig. S3). Although this transition is rare, it clearly shows that the folding pathway is non unique. By repeatedly pulling and relaxing the protein at loading rates equivalent to those used in the experiments [11], we observe an all-or-none unfolding transition of N (Fig. 5). At much lower loading rates, we observe large fluctuations in the molecular extension due to the presence of \mathcal{I} (Fig. 5), a result that is consistent with the simulations in [19]. These features of the force-extension curves could be checked in future single molecule experiments.

The native topology. For each heteropolymer we have determined the topology of \mathcal{I} , i.e. the configuration of the chain in the state \mathcal{I} . Remarkably, we have always obtained a state composed of a compact core whose contacts are mainly native plus a chain that is extended and hence that has few native contacts –see Fig. 4, 7 and 9.

Next, we have investigated the folding mechanism for different matrices of energies E_{ij} that keep the same native topology, i.e. the same chain configuration in N . In most of the cases, we find a three-state behavior where \mathcal{I}

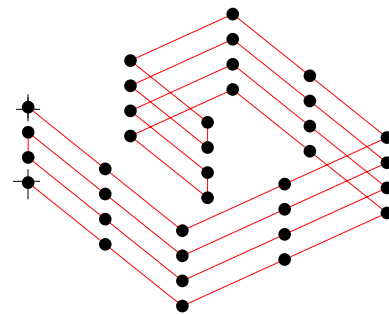


FIG. 6: Example of a structure ($N = 36$) for which we have not observed any three-state mechanism under any conditions.

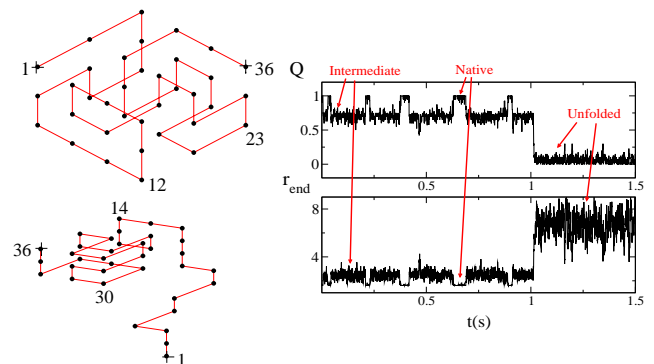


FIG. 7: Example of a structure for which the kinetic barrier between \mathcal{I} and N is smaller than that between \mathcal{I} and S . In this case, during the unfolding transition ($N \rightarrow S$), we can observe a transient regime preceding the transition where the molecule switches between N and \mathcal{I} . $\Delta = 1.09 k_B T^*$ and $f = 9.3 \text{ pN}$. The leftmost lower figure shows a typical configuration of the heteropolymer chain in \mathcal{I} .

shows a structure formed by the same compact core plus an extended random coil (see also Fig. S4 in Supp. Mat.). Because the core, and hence \mathcal{I} , is identical for all cases, this suggests a strong correlation between the three-state behavior and the topology of the native structure, independently of the precise values of the energies E_{ij} . In addition, we have checked that some topologies never lead to the formation of an intermediate state. As an example, the structure shown in Fig. 6 does not lead to a three-state mechanism for any combination of temperature and force values. However, we are not able to give the feature list that must verify a native structure in order to show a force induced three-state behavior in a given range of temperatures. In contrast, as we shall see below, we have found several different structures that show three-state behavior at sufficiently low temperatures.

A versatile intermediate state The experiments on RNase H [11] and our simulations using S_2 suggest that the free energy barrier separating \mathcal{I} and N is higher than the free energy barrier separating \mathcal{I} and S (Fig. 3). This explains that in some range of force and temperature

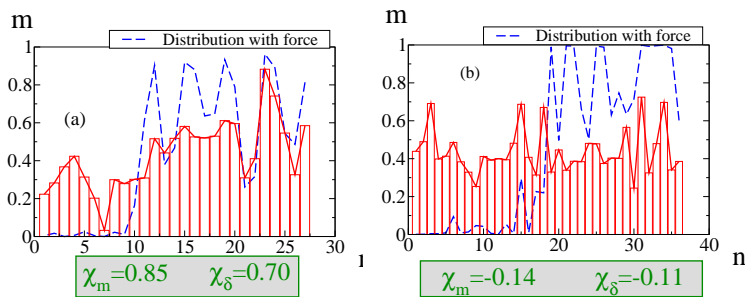


FIG. 8: Average number m of native contacts as a function of the position n of the monomer along the chain. The histograms (in red) correspond to the number of native contacts in the early state (\mathcal{E}) whereas the blue dashed lines correspond to the number of native contacts in \mathcal{I} at (a) $\Delta = 1.43 k_B T^*$, $f = 10.6$ pN for \mathbf{S}_1 and (b) $\Delta = 1.2 k_B T^*$, $f = 9$ pN for \mathbf{S}_2 .

the folding transition to \mathcal{N} starting from \mathcal{S} is preceded by a transient regime where the molecule switches between \mathcal{S} and \mathcal{I} –see Fig. 4. We have found other scenarios where the free energy barrier between \mathcal{N} and \mathcal{I} is smaller than that between \mathcal{S} and \mathcal{I} . In this case we observe, at some force and temperature values, a behavior symmetric to the previous one, i.e. a switching behavior between \mathcal{N} and \mathcal{I} that precedes the unfolding transition from \mathcal{N} to \mathcal{S} –see Fig. 7.

The intermediate state with and without force.

We have investigated whether \mathcal{I} corresponds to the early compact structure \mathcal{E} that forms, starting from a random initial configuration, during the folding at zero force and at the same temperature. We find that sometimes both states are correlated, whereas in other cases they are not.

At zero force, \mathcal{I} is not well-defined since it is not a local minimum along Q or r_{end} . As a consequence, we have used a heuristic method to determine the state \mathcal{E} that has to be compared with \mathcal{I} . The procedure is based on the fact that, in average, Q monotonically tends to 1 during the folding transition. Therefore, for a given random initial condition ($Q \approx 0$), during one folding trajectory at zero force, we record the first configuration that has a value of Q identical to the value of Q in \mathcal{I} . We then define the state \mathcal{E} as the ensemble of these first configurations that are obtained by sampling different random initial conditions and different noise histories. In this ensemble of configurations, we compute the average number m of native contacts for a given monomer as a function of its position n along the chain. The distribution $m(n)$ is then compared to that obtained for \mathcal{I} . The results obtained for the structures \mathbf{S}_1 and \mathbf{S}_2 (Fig. 8) suggest two types of distributions. In Fig. 8a (structure \mathbf{S}_1) the states \mathcal{E} and \mathcal{I} are highly correlated whereas in Fig. 8b (structure \mathbf{S}_2) \mathcal{E} and \mathcal{I} seem to be uncorrelated with each other.

Quantitatively, we measure the correlation between the two structures by computing i) χ_m , the correlation coefficient (also called the Pearson’s correlation coefficient) for the average number of native contacts $m(n)$ and ii) χ_δ

the correlation coefficient for the variation of $m(n)$ along the chain, $\delta(n) = m(n+1) - m(n)$. These are defined by:

$$\chi_m = \frac{N \sum m_i(n) m_e(n) - \sum m_i(n) \sum m_e(n)}{\prod_{k=i,e} \sqrt{N \sum m_k(n) m_k(n) - \sum m_k(n) \sum m_k(n)}},$$

$$\chi_\delta = \frac{N \sum \delta_i(n) \delta_e(n) - \sum \delta_i(n) \sum \delta_e(n)}{\prod_{k=i,e} \sqrt{N \sum \delta_k(n) \delta_k(n) - \sum \delta_k(n) \sum \delta_k(n)}}.$$

The sub-indexes i and e refer to the states that we are comparing, i.e. \mathcal{I} and \mathcal{E} . The sums in χ_m run over all the monomers $n = 1, \dots, N$ whereas the sums in χ_δ run over all the $N - 1$ first monomers. Values of correlation coefficients close to 0 reflect a low correlation between the structures whereas values close to 1 reveal large correlations. Negative values indicate anticorrelation.

We have then investigated, as exhaustively as possible, the native state properties that lead to a similarity between \mathcal{I} and \mathcal{E} . In Fig. 9, we report four examples of such structures that show a three-state behavior and that have different degrees of similarity between \mathcal{I} and \mathcal{E} .

Why we expect the states \mathcal{I} and \mathcal{E} to differ? First of all, during the folding at zero force the monomers tend to form native contacts independently of their position along the polymer chain. In contrast, the intermediate state with force has the core/extended-chain structure described above that is energetically favored due to the stretching effect of the force. Despite of this difference, most of the structures we investigated show a strong correlation (χ_δ biased towards 1) for the variation $\delta(n)$ of the average number of native contacts (see Figs. 8, 9).

Next, we have observed that monomers in \mathcal{I} tend to locally form crankshafts (see Figs. 4 and 9. see also the illustration shown at the beginning of Section I for the shape of a crankshaft). Moreover, structures with a high similarity between \mathcal{I} and \mathcal{E} also show a fairly high content of monomers that form crankshafts in \mathcal{N} (see for instance the structures \mathbf{S}_2 in Fig. 2 and the structures in Fig. 9a, Fig. 9b and Fig. 9d). A crankshaft arrangement of monomers reflects the formation of non-covalent bonds between monomers that are close to each other along the polymer chain. From the point of view of real proteins, this would suggest that the interaction of sub-units that are close to each other along the amino acid chain is necessary for \mathcal{I} and \mathcal{E} to be similar.

On and off-pathway states. The extension trace of Fig. 4 (see also Fig. S5 and Fig. S6 in Supp. Mat.) shows that the last folding step starts from \mathcal{I} . A similar observation has led Ceconi *et. al* to argue that \mathcal{I} is on-pathway. However, we cannot discard the possibility of the presence of additional intermediate states off-pathway having the same molecular extension, i.e. misfolded states (Fig. 1). We then propose the following

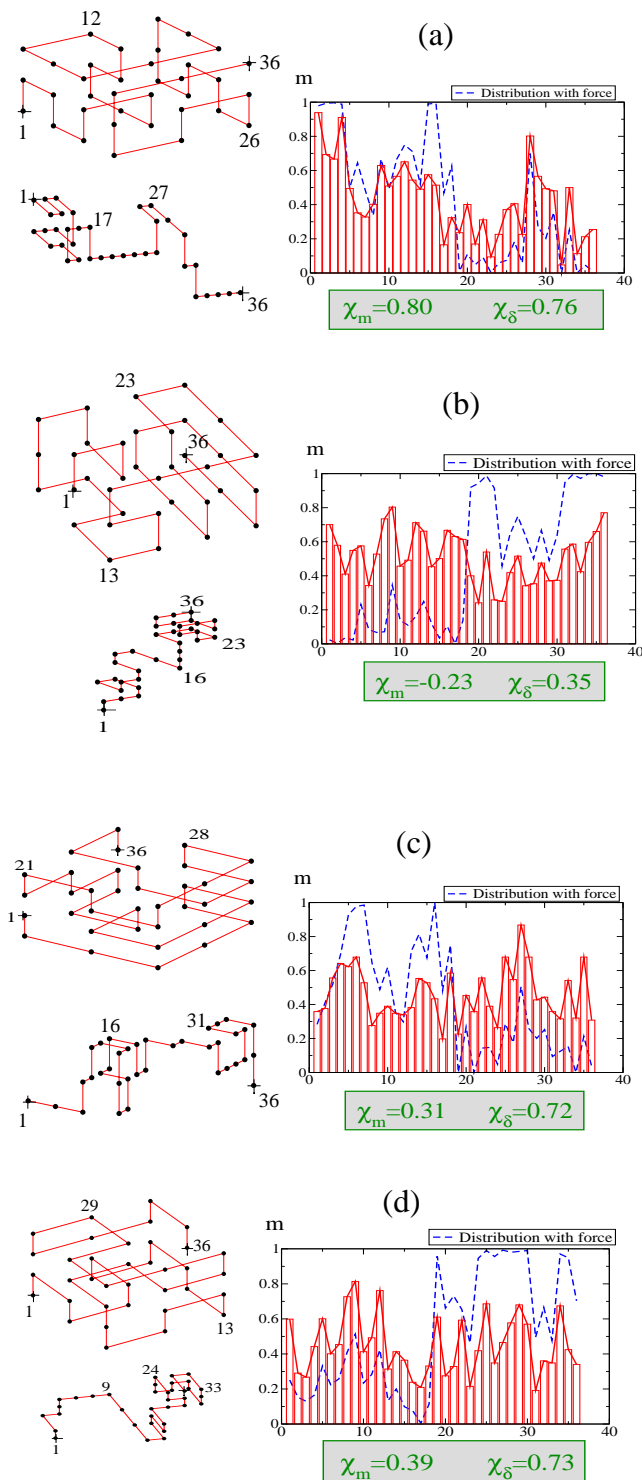


FIG. 9: Four examples of structures showing a three-state behavior and having different degrees of correlation between \mathcal{I} and \mathcal{E} . For each figure, the upper panel on the left shows the native structure whereas the lower panel on the left shows a typical configuration of the heteropolymer chain in \mathcal{I} . Fig 9a: $\Delta = 1.09 k_B T^*$ and $f = 7.6$ pN. Fig 9b: $\Delta = 1.09 k_B T^*$ and $f = 6.7$ pN. Fig 9c: $\Delta = 1.14 k_B T^*$ and $f = 7.5$ pN. Fig 9d: $\Delta = 1.09 k_B T^*$ and $f = 7.2$ pN.

experimental force jump protocol to detect and quantitatively measure the fraction of misfolded states. Each time the system folds into \mathcal{I} , we relax the force to zero and compute the distribution of folding times. In the presence of misfolded states, one should get a bimodal distribution composed of a short-time contribution corresponding to on-pathway states and a long-time tail corresponding to off-pathway states. Indeed, misfolded states are expected to be separated from \mathcal{N} by high energy barriers that slow down the folding dynamics leading to large folding times [8, 30].

We have carried out numerical simulations of this force jump protocol (i.e. we relax the force to zero once the system has a number of contacts corresponding to \mathcal{I}) in two cases: when only on-pathway intermediate states are present and when a mix of on-pathway and off-pathway states are present. In most cases we studied we found that \mathcal{I} was on-pathway. A convenient way to generate misfolded states is to consider a structure showing only on-pathway states and then add solvent conditions that favor the formation of misfolded states. We include the effect of hydrophobic interactions between the amino acid side chains of a protein and the water molecules in solution by introducing an additional energy term e_h for each interaction between a molecule of the solvent (corresponding to a free node on the lattice) and a monomer. The overall energy contribution for a monomer is $p e_h$ where p is the number of nearest neighbor free nodes of that monomer. $e_h > 0$ favors hydrophobicity by increasing the interactions between the monomers. For the sake of simplicity, we have taken a single value of e_h for all monomers. However, one could do more general and introduce a value of e_h for each individual monomer by adding specific (positive or negative) contributions to control the degree of hydrophobicity of each monomer. The latter procedure has been used to model the effect of a denaturant on the folding transition [27].

Fig. 10 reports the distribution of folding times for \mathbf{S}_1 that shows the presence of misfolded states. Without hydrophobicity ($e_h = 0$), the temperature and force values used are such that there are only on-pathway states, thus leading to a smooth monotonic distribution of folding times. By adding hydrophobicity, i.e. $e_h > 0$, monomers tend to interact more with each other. Although the temporal evolution of r_{end} is similar to that observed in the $e_h = 0$ case, we actually obtain a mixture of on-pathway and off-pathway states. The former contributes to the short time distribution of Fig. 10 whereas the latter corresponds to the contribution at very large times. By separately integrating out each part of the distribution, we are able to measure the fraction of on/off-pathway trajectories that lead to on/off pathway states respectively. For the example shown in Fig. 10, we get $42\% \pm 5\%$ and $58\% \pm 5\%$ of on/off-pathway folding trajectories respectively. Force jump protocols could be implemented in optical tweezers and AFM experiments to measure the fraction of on/off-pathway folding trajectories.

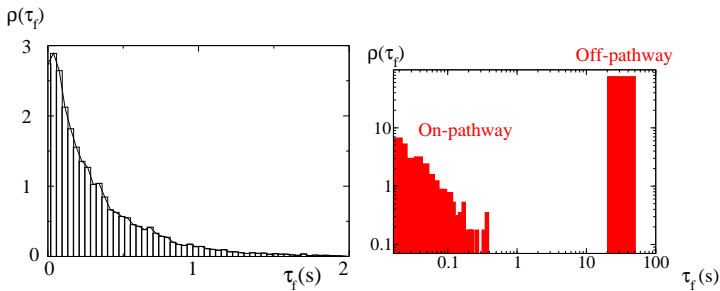


FIG. 10: Left panel: Distribution of folding time τ_f after setting the initial force to zero once \mathcal{I} is reached in the absence of hydrophobic effects for the structure \mathbf{S}_1 with $\Delta = 1.7 k_B T^*$ and $f = 13.2$ pN. In this case, we observe only on-pathway states. Right panel: Same distribution of folding time τ_f but in the presence of hydrophobic effects that lead to off-pathway intermediate states. The values are $\Delta = 1.67 k_B T^*$, $f = 13.2$ pN and $e_h = 0.5 k_B T$. The rightmost vertical bar counts for trajectories that have $\tau_f > 20$ s. Because the size of the systems we run our simulations is small, when \mathcal{I} is reached we constrain the system to keep a number of native contacts larger than those in \mathcal{I} . In this way we reduce finite-size effects and obtain a clear separation of timescale between on-pathway and off-pathway states.

II. EXPERIMENTAL PROTOCOLS AND THE INTERMEDIATE STATE

Determining the structure of non-native states of nucleic acids and proteins remains a major experimental challenge in modern biophysics. For instance, even the structure of the denatured state of the lysozyme protein that has been studied over half a decade is still unresolved [28]. In this regard, the use of single-molecule techniques appears as a promising tool to identify kinetic pathways and intermediate states [4]. In this section, we propose specific protocols in single molecule pulling experiments aiming to determine, within *one* amino acid accuracy, the location of the core in proteins with an intermediate state. Implementation of these protocols require well known methodologies in protein biophysics.

A useful method to determine the structure of \mathcal{I} consists in measuring the unfolding/folding kinetic rates, k_u and k_f , associated to the transition $\mathcal{I} \leftrightarrow \mathcal{S}$ after modifying the protein in various ways. These rates are obtained by recording, at a given force, the molecular extension of the protein and measuring the inverse of the average residence time of the protein in each state \mathcal{I} and \mathcal{S} (see Fig. 4).

A " ϕ -value" force protocol. A possible modification of the protein consists in selectively mutating an individual amino acid. The idea of this method is reminiscent of the ϕ -value technique used in bulk measurements [29]. In our case, we consider a heteropolymer where initially $e_h^i = 0$ for all i . We then select one monomer i and assign new values for the interaction energies E_{ij}

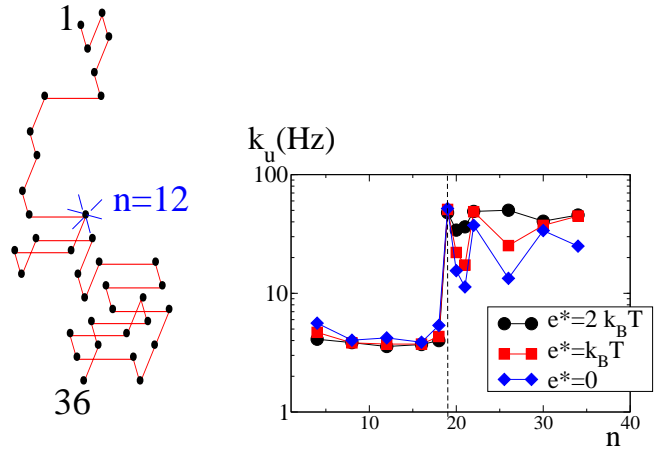


FIG. 11: Point mutation protocol. Left: Unstructured intermediate configuration. The star indicates a mutated amino acid. Right: k_u a function of the location n of the mutation along the chain for different values of the hydrophobicity of the mutated monomer, e^* . The structure is \mathbf{S}_2 , $\Delta = 1.2 k_B T^*$ and $f = 9$ pN. The dashed line indicates the position of the first monomer ($n_f = 19$) inside the core. The core is composed of all the monomers that follow up from that monomer until the end of the chain.

between that monomer and the other monomers j of the chain. We also increase the degree of hydrophobicity of that monomer i by setting $e_h^i = e^* > 0$ while keeping the rest of the e_h^i 's equal to zero. In Fig. 11 we report for \mathbf{S}_2 the values of k_u as a function of the location n of the mutation along the chain and for different values of e^* . One can clearly see a transition separating low and high rates that is distinctly located at the edge of the core. Low rates correspond to mutations on the free chain whereas high rates correspond to mutations inside the core. The larger e_h , the sharper the transition, which suggests the use of very hydrophilic amino acids, such as serine or threonine as point mutations.

From an experimental point of view, a single mutation may not be sufficient to distinguish a transition because of the too small differences in the rates. We then suggest a multiple-points mutation analysis: instead of mutating a single amino acid, two or more successive amino acids can be mutated. This helps to identify more clearly the transition but also leads to a less precise location of the position of the edge of the core (Fig. S7 in Supp. Mat.).

Cutting the proteins. According to Kramers-Bell theory, the transition rates between \mathcal{I} and \mathcal{S} depend exponentially on the applied mechanical force, showing a chevron-like shape [5] – see Fig. 12. In these kind of plots we represent the unfolding (k_u) and folding (k_f) rates as a function of force. Therefore, the increasing (respectively decreasing) curves correspond to the dependence of the rates k_u (respectively k_f) of the transition $\mathcal{I} \rightarrow \mathcal{S}$ (respectively $\mathcal{S} \rightarrow \mathcal{I}$). The crossing point of a chevron

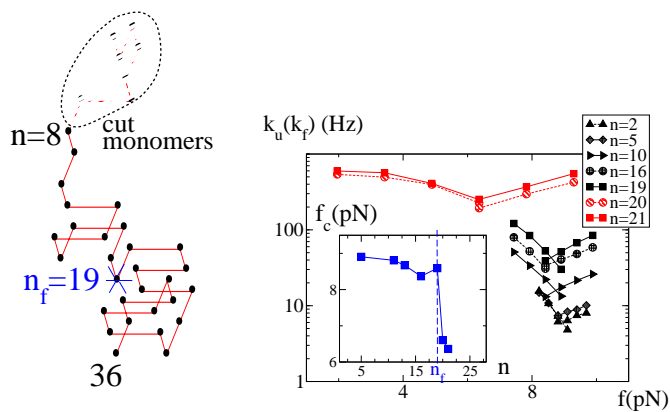


FIG. 12: Cutting protocol. Left: Unstructured intermediate configuration. The black dashed circle indicates the cut in the chain. Cutting at the monomer n along the heteropolymer means “removing the monomers 1, 2, ..., $n-1$ ”. Right: We report the values of the “unfolding” and “folding” rates for the reaction $\mathcal{I} \leftrightarrow \mathcal{S}$ as a function of the applied force f , which leads to the so-called chevron plots. The different chevron plots correspond to different locations of the cutting of the heteropolymer. The structure is \mathbf{S}_2 with $\Delta = 1.2 k_B T^*$. Insets: Critical forces as a function of the cutting position n . The vertical dashed line marks the position of the first monomer ($n_f = 19$) that separates the core from the extended chain. We find that, at n_f , the value of the critical force (where unfolding and folding rates are equal) suddenly drops (compare the chevron plots for $n = 19$ (black) and $n = 20$ (red)).

plot ($k_u = k_f$) is located at the value of the force where both rates ($\mathcal{I} \rightarrow \mathcal{S}$ and $\mathcal{S} \rightarrow \mathcal{I}$) are identical. This is the critical force where the two species (\mathcal{I} and \mathcal{S}) are equally probable. We have measured these rates in \mathbf{S}_1 and \mathbf{S}_2 after cutting off the extremities of the chains at certain locations, i.e. leading to a shorter polypeptide chain. Fig. 12 shows the chevron plots for \mathbf{S}_2 as we keep the extremity fixed at one end of the core and progressively reduce the length of the chain. We see a sharp transition, characterized by a drop of the critical force (insets of Fig. 12), when the cut is done inside the core. In this case, \mathcal{I} loses its stability because of the spoiling of the core, a rather intuitive result. This allows again to locate the core with one monomer accuracy. Other similar modifications where protein interactions are changed are shown in Fig. S8 in the Supp. Mat..

Circular permutations. Circular permutations are useful modifications that allow to investigate the stability of native structures. In this case, new polypeptide chains are obtained by shifting all the amino acids in the original chain by a certain amount a . An amino acid at the position i will then go to the position $i + a$ (modulo the number of amino acids in the protein) where a can be positive or negative. We have measured the rates k_u and k_f in heteropolymers obtained by circular permutations

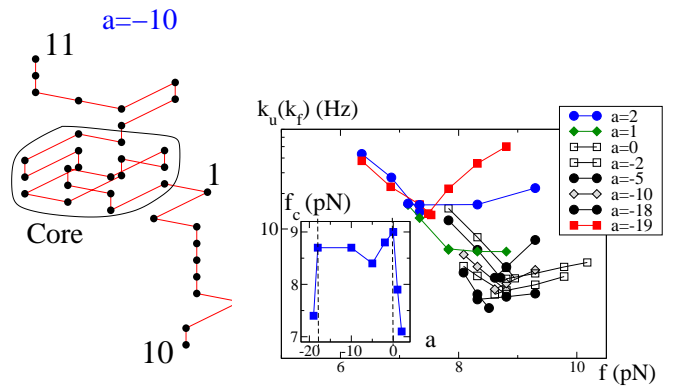


FIG. 13: Permutation protocol. Left: Unstructured intermediate configuration after circularly permuting \mathbf{S}_2 by $a = -10$. The numbers indicate the initial position of the monomers in \mathbf{S}_2 . Right: Chevron plots for circular permutations of \mathbf{S}_2 by a . $\Delta = 1.2 k_B T^*$. Inset: Critical forces as a function of a . The vertical dashed lines indicate a values where the core dissociates.

of \mathbf{S}_2 . We find, again, transitions when the circular permutation dissociates the core. The two transitions are found at both edges of the core (right and left, see Fig. 13) and are characterized by a sudden drop in the critical force.

We have finally investigated an experimental protocol in which we change the location of the applied force along the chain. In this case, the presence of undesired interactions involving the monomers that are not pulled by the force makes difficult the analysis of the traces. The traces are indeed noisy due to the formation of new states that are very unlikely when stretching from the very ends of the heteropolymer. The important problem about how mechanical unfolding depends on the location of the force entails a more detailed study that we do not pursue here.

III. CONCLUSION

In many respects designed on-lattice heteropolymers are crude approximations to real proteins. Yet, it seems again, that these models share common features with the folding of single-domain proteins. In particular these models seem appropriate to investigate the three-state behavior that has been recently observed in single-protein force experiments [11]. What is the link between the present lattice model results and real wild-type proteins? It is important to make clear the limitations of the current approach. Although most of our study has been inspired by recent results in RNaseH it remains a challenge to establish a clear connection between the native three dimensional structure of a real protein and the topology of the native structure used in heteropolymer models. Let us stress that lattice models are phenomenological

models useful to design specific free energy landscapes capable of reproducing different kinetic scenarios for folding (e.g two-states, three-states, intermediate states on/off pathway, correlated/uncorrelated early and intermediate states and so on). From this perspective we expect that the phenomenology described here is quite general and probably observed in proteins other than RNase H.

Interestingly, the stabilization by mechanical force of a unique intermediate state suggests possible ways to experimentally infer its structure. We have found that this state is composed of an unstructured and stretched part of the polypeptide chain plus a rigid core that corresponds to some part of the native state. This result might be specific to the details of the model, yet the competition between different types of low entropy regions along the polypeptide chain (a compact core versus an extended chain) could be reasonably argued to be the generic driving force for the formation of unstructured extended chains. It must be emphasized, however, that our model does not include side chain interactions. These are known to induce a large entropy loss upon folding due to the excluded volume interactions present in the packed native state [31, 32]. Therefore we cannot exclude a scenario where the large entropy of the side chains might induce a molten globule like intermediate state in force where the protein keeps a single native-like core with freely moving side chains[33]. Our simulations also reveal (see Fig. S10) that the presence of a rigid core is not necessarily correlated with the hydrophobicity of the monomers in the chain. This suggests that, although amino acid composition can facilitate the formation of a core, an excess of hydrophobic monomers is not a necessary requirement for its formation.

Although real proteins are too complex to be modeled

with "beads and sticks in regular lattices", these models are useful to infer possible experimental protocols to probe the intermediate state. The experimental protocols we propose in this work (point mutations, cutting the polypeptide chain and circular permutations) are well known in protein biophysics and could be used to distinguish between a molten globule and an unstructured extended state. Indeed, if these modifications of the protein lead to the same types of transitions as in Fig. 11, 12, 13, it is likely that the intermediate state is composed of a core plus an unstructured extended chain. In the case of a uniform dependence of the rates this would suggest that the intermediate state resembles more a molten-globule structure where no rigid core is present. More generally, these techniques could be applied to precisely determine the location of the disordered and ordered domains in unstructured proteins.

Finally we have shown that force measurements can also be used to highlight the presence of misfolded states, and to quantify the relative fraction of on/off-pathway trajectories. From this perspective force measurements suggest the possibility of probing the shape of the free energy landscape in proteins and investigating the glassy behavior of proteins at low temperatures [34, 35, 36].

Acknowledgments

We are grateful to C. Bustamante, C. Cecconi, M. Manosas and S. Marqusee for useful suggestions. I. J acknowledges financial support from the European network STIPCO, Grant No. HPRNCT200200319. F. R acknowledges financial support from the Ministerio de Educación y Ciencia (Grant FIS2004-3454 and NAN2004-09348) and the Catalan government (Grant SGR05-00688).

-
- [1] Ishijima, A. & Yanagida, T. (2001) *Trends Biochem. Sci.* **26**, 438-444.
- [2] Fisher, T. E., Piotr, M. E. & Fernandez, J. M. (2000) *Nat. Struct. Biol.* **7**, 719-724.
- [3] Weiss, S. (2000) *Nat. Struct. Biol.* **7**, 724-729.
- [4] Ritort, F. (2006) *J. Phys.: Condens. Matter* **18** R531-R583.
- [5] Finkelstein, A. V. & Ptitsyn, O. B. (2002) *Protein Physics* (Soft condensed matter complex fluids and biomaterial series, Academic Press).
- [6] Junier, I. & Ritort, F. (2006) *AIP Conference Proceedings*, **851**, 70-95.
- [7] Fersht, A. R. & Daggett, V. (2002) *Cell* **108**, 573-582.
- [8] Onuchic, J. N. & Wolynes, P. G. (2004) *Curr. Op. Struct. Biol.* **14**, 70-75.
- [9] Marszalek, P. A. Lu, H., Li, H., Carrion-Vazquez, M., Oberhauser, A. F., Schulten, K. & Fernandez, J. M. (1999) *Nature* **402** 100-103.
- [10] Williams, P. M. Fowler, S. B., Best, R. B., Toca-Herrera J. L., Scott, K. A., Stewart, A. & Clarke, J. (2003) *Nature* **422** 446-449.
- [11] Cecconi, C., Shamk, E. A., Bustamante, C. & Marqusee, S. (2005) *Science* **309**, 2057-2060.
- [12] Kuzmenkina, E. V., Heyes, C. D. & Nienhaus, G. U. (2006) *J. Mol. Biol.* **357**, 313-324.
- [13] Kuzmenkina, E. V., Heyes, C. D. & Nienhaus, G. U. (2005) *Proc. Natl. Acad. Sci. USA* **102**, 15471-15476.
- [14] Raschke, T. M. & Marqusee, S. (1999) *Nat. Struct. Biol.* **6**, 825- 831.
- [15] Daggett, V. & Fersht, A. R. (2003) *Trends Biochem. Sci.* **28**, 18-25.
- [16] Dyson, H. J. & Wright, E. (2005) *Nat. Rev. Mol. Cel. Bio.* **6**, 197-208.
- [17] Shakhnovich, E. I. & Gutin, A. M. (1993) *Proc. Natl. Acad. Sci. USA* **90**, 7195-7199; Shakhnovich, E. I. (1994) *Phys. Rev. Lett.* **72**, 3907-3910.
- [18] Socci, N. D., Onuchic, J. N. & Wolynes, P. G. (1999) *Proc. Natl. Acad. Sci. USA* **96**, 2031-2035.
- [19] Klimov, D. K. & Thirumalai, D. (1999) *Proc. Natl. Acad. Sci. USA* **96**, 6166-6170; Klimov, D. K. and Thirumalai, D. (2001) *J. Phys. Chem. B* **105**, 6648-6654.
- [20] Hillorst, H. J. and Deutch, J. M. (1975) *J. Chem. Phys.* **63**, 5153-5161.
- [21] Onuchic, J. N., Wolynes, P. G., Luthey-Schulten, Z. &

- Socci, N. (1995) Proc. Natl. Acad. Sci. USA **92**, 3626-3630.
- [22] Shakhnovich, E. I. (1997) Curr. Opin. Struct. Biol. **7**, 29-40.
- [23] Chan, H.S & Dill, K. A. (1989) J. Chem. Phys., **90**, 492-509.
- [24] Rief, M., Gautel, M., Oesterhelt, F., Fernandez, J. M. & Gaub H. E. (1997) Science **276**, 1109-1112.
- [25] Liphardt, J., Onoa, B., Smith, S. B., Tinoco, I., Jr., Bustamante, C. (2001) Science **292**, 733-737.
- [26] Muñoz, V. & Sanchez-Ruiz, J. (2004) Proc. Natl. Acad. Sci. USA **101**, 17646-17651.
- [27] Pande, V. S. & Rokhsar, D. S. (1998) Proc. Nat. Acad. Sci. USA **95**, 1490-1494.
- [28] Fitzkee, N. C. & Rose, G. R. (2004) Proc. Natl. Acad. Sci. USA **101**, 12497-12502.
- [29] Fersht, A. R., Leatherbarrow, R. J. & Wells, T. N. C. (1986) Nature **322**, 284-286.
- [30] Gutin, A., Sali, A., Abkevich, V., Karplus, M. & Shakhnovich, E. I. (1998) J. Chem. Phys. **108**, 6466-6483.
- [31] Broomberg, S. & Dill, K. A. (1994) Protein Sci. **3**, 997-1009
- [32] Klimov, D. K. & Thirumalai, D. (1998) Folding & Design **3**, 127-139.
- [33] Shakhnovich, E. I. & Finkelstein, A. V. (1994) Biopolymers **28**, 1667-1680.
- [34] Bryngelson, J. D. & Wolynes, P. G. (1987) Proc. Natl. Acad. Sci. USA **84**, 7524-7528.
- [35] Hyeon, C. & Thirumalai, D. (2003) Proc. Natl. Acad. Sci. USA **100**, 10249-10253.
- [36] Brujić, J., Hermans Z., R. I., Walther, K. A. & Fernandez, J. M. (2006) Nature Physics **2**, 282-286.